Tailored Dealloying Products of Cu-based Metallic Glasses in Hydrochloric Acid Solutions

Zhifeng Wang, Lijuan Wang, Chunling Qin*, Jiangyun Liu, Yongyan Li, Weimin Zhao

School of Materials Science and Engineering, Hebei University of Technology, Tianjin 300130, China

Free dealloying of Cu-Hf-Al metallic glasses in HCl electrolytes are studied in this paper. The results show that the electrolyte concentration and dealloying time strongly influence the type of dealloying products. A superficial dealloying happens in diluted HCl electrolytes while a complete dealloying occurs in concentrated HCl electrolytes. The results present that Cu_2O microparticles with regular morphology can be tailored on glassy surfaces in 0.05 M HCl solution by controlling the dealloying time. Furthermore, the designable products of nanoporous Cu, Cu_2O nanoplates and CuO microwires can be fabricated in 1.2 M HCl electrolyte with the dealloying time. Due to a big difference of examined Cu-Hf-Al alloys in the electrolyte concentration and dealloying time, one or mixed dealloying products (Cu, Cu_2O and CuO), which depend on the progress of relative chemical reactions and the different dealloying route, will finally be produced.

Keywords: *Metallic glass, dealloying, corrosion products, hydrochloric acid*

1. Introduction

Dealloying, or selective removal of one or more components from a binary or multicomponent alloy, has become a popular technique for rapid and direct generation of various nanoporous metals and alloys recently[1-4]. Nanoporous metals produced by dealloying have been applied in many fields, such us catalysis[5], heat exchangers[6], actuators[7], energy storage[2,8], fuel cells[9], sensors[10] and radiation damage resistant materials[11]. Moreover, dealloying process can be extended to the fabrication of important transition metal oxide nanostructures with intricate structural properties rather than a porous structure as often seen during dealloying[12]. For instance, regular Fe_3O_4 octahedra, Co_3O_4 nanoplates and octahedral-like Mn_3O_4 nanoparticles have been successfully produced by the in situ dealloying and spontaneous oxidation method[13,14]. Nowadays, not only nanoporous metals but also transition metal oxide can be fabricated by dealloying and extended methods.

Usually, the formation of a porous structure during dealloying in electrolytes needs to address some issues including the critical potential, the dealloying threshold, the initial alloy composition and so on[15]. Furthermore, Chen[16] found that a critical concentration of electrolytes required for the formation of nanoporosity. For example, nanoporous Cu (NPC) with different pore characteristics are able to be fabricated by electrochemically dealloying $Cu_{30}Mn_{70}$ alloy in 0.025 M, 0.1 M and 0.5 M HCl electrolytes with different time. Instead of the formation of NPC, however, nanostructured cuprous oxide (Cu_2O) is made on the ribbon surfaces when electrochemically dealloying of the same alloy in 0.001 M HCl solution. Therefore, we can see that the electrolytes concentration is one of the key factors to determine which kind of dealloying products can be created during the dealloying.

Up to now, lots of literatures have focused on the fabrication of nanoporous Cu by dealloying different precursors in HCl solutions[17-19]. Unfortunately, few studies focused on the other dealloying products obtained from these precursors in HCl solutions[20,21]. In this paper, in order to systematically investigate the correlation between the dealloying products and the dealloying conditions, free dealloying of Cu-Hf-Al metallic glasses in both diluted and concentrated HCl electrolytes for different time are carried out. Various dealloying products, including NPC, Cu_2O, and CuO with interesting morphologies, are produced and tailored by controlling the dealloying conditions. The in-depth understanding the chemical process during dealloying is discussed in this work, which guides for designing different useful dealloying products.

2. Experimental

Ternary alloys with nominal compositions of $Cu_{52.5}Hf_{40}Al_{7.5}$ (at.%) were prepared by arc melting a mixture of pure Cu (99.99 wt.%), pure Hf (99.99 wt.%) and pure Al (99.99 wt.%) in a high-purity argon gas atmosphere and using Ti getters. The melt spinning method was used to prepare amorphous Cu-Hf-Al ribbons with 20 μm in thickness and 2 mm in width.

Dealloying was performed in hydrochloric acid (HCl) solutions with a concentration of 0.05 M and 1.2 M in a free corrosion condition open to air at 298 K. After different immersion times, the dealloyed ribbons were taken out and well rinsed with deionized water for three times to remove the residual chemical reagents and then dried in a vacuum drying oven before a further testing.

The amorphicity of the as-spun Cu–Hf–Al sample and phase type of the dealloyed specimens were confirmed by X-ray diffractometer (XRD, Bruker D8) with Cu Kα

*e-mail: chunlingqin@163.com; clqin@hebut.edu.cn

radiation (λ = 0.15418 nm). The morphology of the as-dealloyed samples was observed by scanning electron microscope (SEM, Hitachi S-4800). The volume fraction of the dealloying products, which means the surface coverage rate of the corrosion products (such as Cu_2O and CuO particles), is measured by the software Image Tool.

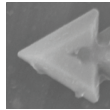## 3. Results and Discussion
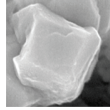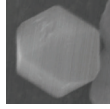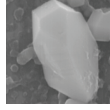
3.1. *Dealloying in 0.05 M HCl solution*
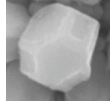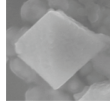
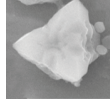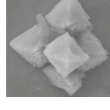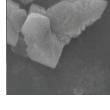Figure 1 shows SEM images of the $Cu_{52.5}Hf_{40}Al_{7.5}$ metallic glasses dealloyed in 0.05 M diluted HCl solution at 298 K for different time. Regular Cu_2O particles identified by XRD and energy-dispersive spectroscopy analysis[20,21] with various shapes are formed on the surfaces of glassy alloys. With the increase of the dealloying time, Cu_2O crystals with shapes of truncated tetrahedron (4 h, Figure 1a), cube (5 h, Figure 1b), cuboctahedron (6 h)[20], elongated cuboctahedron (7 h, Figure 1c), truncated octahedron (8 h)[20], octahedron (14 h, Figure 1d), hexapods (20 h) and dendrite (24 h)[20] are observed on the ribbon surfaces. It is the first systematic work to synthesize Cu_2O crystals with various shapes successfully by dealloying method. As a result, regular Cu_2O microparticles with designable morphology can be tailored in diluted HCl solutions by controlling dealloying time.

Characteristics including morphology, size and volume fraction of Cu_2O crystals produced by free dealloying of $Cu_{52.5}Hf_{40}Al_{7.5}$ glassy alloys in 0.05 M HCl solution for different time open to air at 298 K are summarized in Table 1. From the Table 1, it can be seen that the three-dimensional sizes of Cu_2O crystals do not change much in the first 8 hours of dealloying though they show different edge length. Then, the sizes of Cu_2O crystals increase obviously after dealloying for 14 h, and get bigger with the increase of the dealloying time. It should be noted that, in this work, the volume fraction of Cu_2O particles on the surface is low (less than 20%) and does not change much with the extension of etching time. Since the Cu_2O crystals with different morphologies possess interesting physical, electrical and optical properties[22-24], it is important to enhance the volume fraction of Cu_2O particles on the glassy surface. Furthermore, metallic glasses are good carriers for Cu_2O particles due to their high strength and high toughness. In the future, the as-prepared metallic glass/Cu_2O compounds with multiple properties are hopeful to be applied in broad fields.

3.2. *Dealloying in 1.2 M HCl solution*

XRD patterns of the $Cu_{52.5}Hf_{40}Al_{7.5}$ metallic glasses etched in 1.2 M concentrated HCl solution open to air at 298 K for different time are shown in Figure 2. The diffraction pattern for the as-spun alloy (dealloying for 0 h) exhibits a broad halo peak and has no Bragg peaks (Figure 2a), indicating a single homogeneous glassy structure. However, the broad peak disappears after dealloying for 12 h or longer time, which demonstrates that glassy structure is destroyed for the $Cu_{52.5}Hf_{40}Al_{7.5}$ metallic glasses dealloyed in concentrated HCl solution for a long time. When dealloying for 12 h, Figure 2b reveals that only peaks matching with

Table 1. Characteristics of Cu_2O crystals produced by free dealloying of $Cu_{52.5}Hf_{40}Al_{7.5}$ glassy alloys in 0.05 M HCl solution for different time at 298 K open to air.

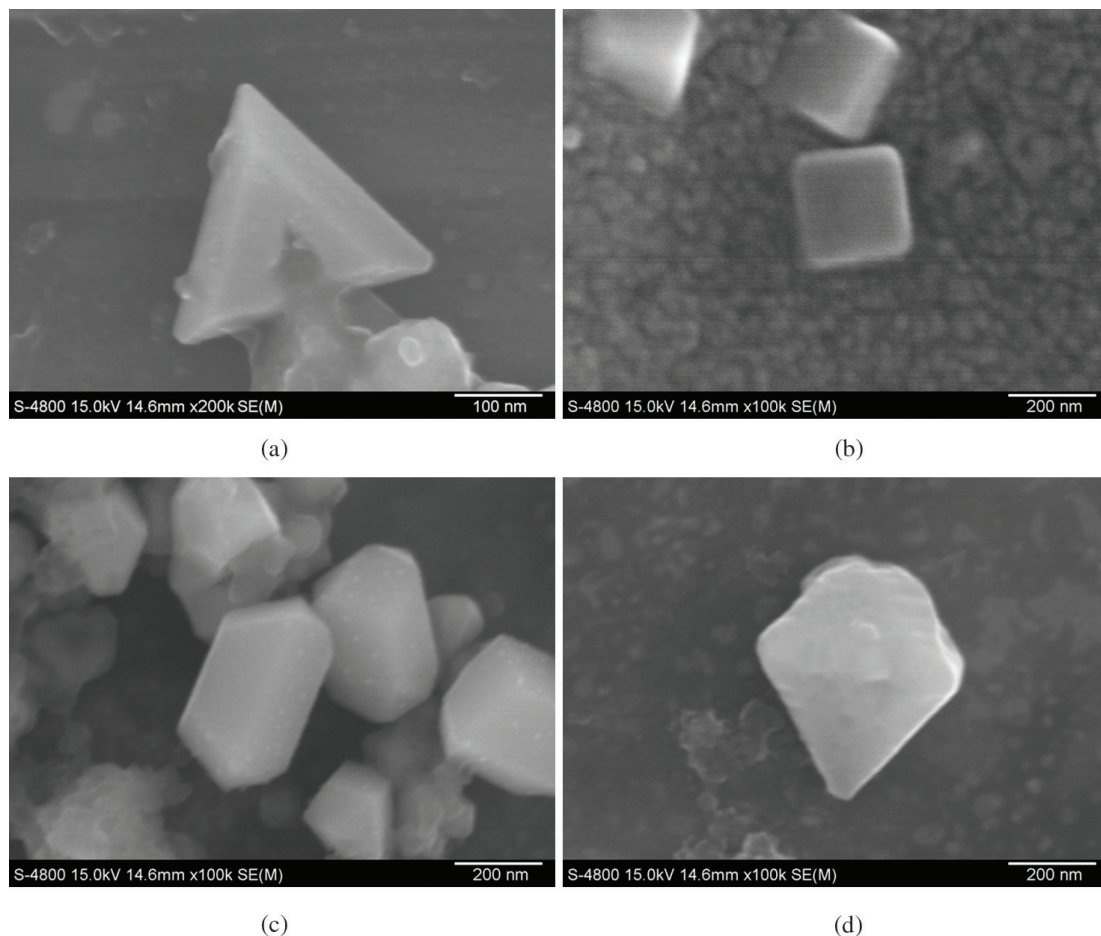| Dealloying time/h	4	5	6	7	8	14	20	24	
Morphology									
	Truncated tetrahedron	Cube	Cuboctahedron	Elongated cuboctahedron	Truncated octahedron	Octahedron	Hexapods	Octahedron-detached hexapods	Dendrite
Edge length/nm	~300	~300	~300	~200	~150	~450	~500	~1100	~1400
Volume fraction/%	10.6	13.3	12.2	13.7	13.9	15.8	14.4	5.5	14.3
								Total: 19.8	
References	This work	This work	[20]	This work	[20]	This work	[20]	[20]	[20]

Figure 1. SEM images of the $Cu_{52.5}Hf_{40}Al_{7.5}$ metallic glasses etched in 0.05 M HCl solution at 298 K for (a) 4 h, (b) 5 h, (c) 7 h, (d) 14 h.

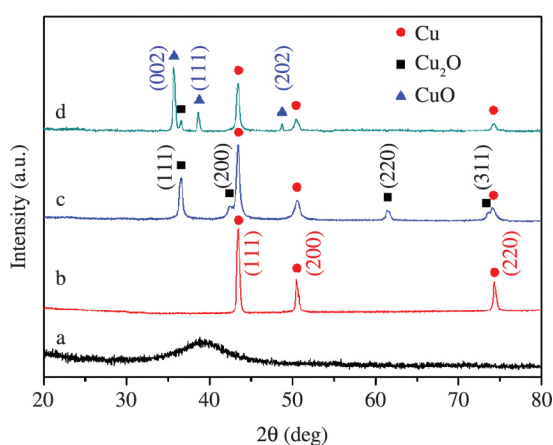**Figure 2.** XRD patterns of the $Cu_{52.5}Hf_{40}Al_{7.5}$ metallic glasses etched in 1.2 M HCl solution at 298 K for (a) 0 h, (b) 12 h, (c) 14 h, (d) 18 h.

fcc Cu (111), (200) and (220) (JCPDS number 04-0836) are obtained, and no peaks corresponding to Hf and Al elements are observed. The results indicate that the Hf and Al elements are removed from the alloy precursor, while

the dealloying process is nearly complete. In addition, the crystal peaks in Figure 2c match with (111), (200), (220) and (311) crystal planes of Cu_2O (JCPDS number 05-0667) besides (111), (200) and (220) crystal planes of Cu. Thus, according to the increase of dealloying time from 12 h to 14 h, respectively, the dealloying products change from Cu to Cu_2O/Cu compounds. Furthermore, after dealloying for 18 h, it can be seen that (002), (111) and (202) crystal planes of CuO (JCPDS number 89-5899), (111) crystal planes of Cu_2O and (111), (200) and (220) crystal planes of Cu can be identified from the XRD patterns shown in Figure 2d. Accordingly, the corrosion products with CuO/Cu_2O/Cu mixture are made on the $Cu_{52.5}Hf_{40}Al_{7.5}$ alloy surface after dealloying in 1.2 M concentrated HCl solution for 18 h. On the other hand, from Figure 2(b)-(d), we can also see that the relative intensity of Cu peak decreases with the increase of the dealloying time, indicating that the dealloying product Cu has gradually transformed to Cu_2O and/or CuO during the dealloying.

SEM images of the $Cu_{52.5}Hf_{40}Al_{7.5}$ metallic glasses etched in 1.2 M HCl solution for different time are shown in Figure 3. Considering XRD results, as shown in Figure 2b, it is interestingly found that a nanoporous Cu structure in Figure 3a is produced by the accumulation
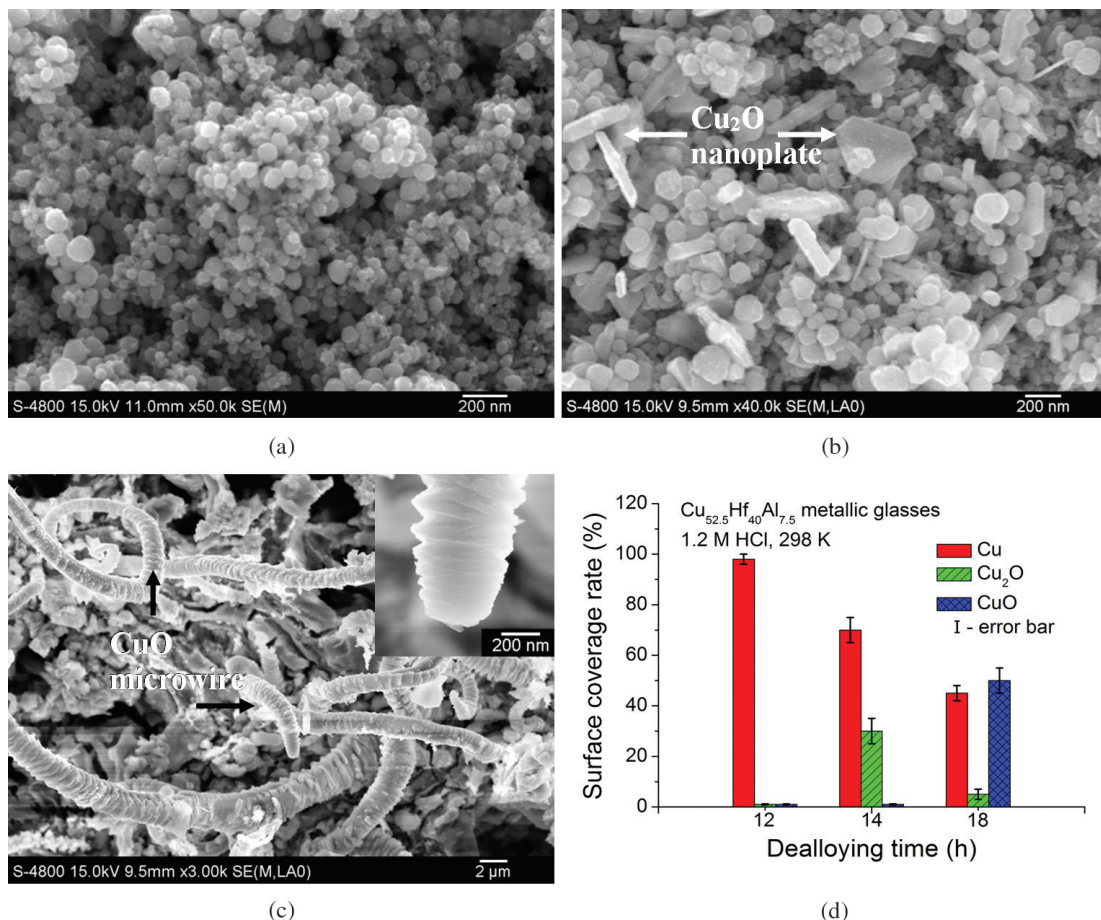
Figure 3. SEM images of the $Cu_{52.5}Hf_{40}Al_{7.5}$ metallic glasses etched in 1.2 M HCl solution at 298 K for (a) 12 h, (b) 14 h, (c) 18 h, the inset shows the microwire image at a higher magnification. (d) Surface coverage rate of different corrosion products with dealloying time.
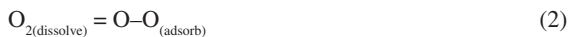
of Cu nanospheres with diameter of 70-90 nm during the 12-hour dealloying. In this situation, a complete dealloying has finished, which results from relatively high concentration of HCl electrolytes and long time of etching (12 h). We should note that the as-produced nanoporous structure shown in Figure 3a is not the same as the widely studied bicontinuous nanoporous structure during dealloying[25]. The different dissolution behavior of constituent elements in dealloying electrolytes seems to be an important factor to influence the reorganized way of residual noble metal during the dealloying. There must be complicated reasons for determining the type of NPC, which would arouse an interesting topic for discussion.
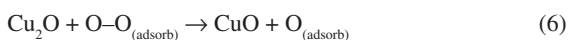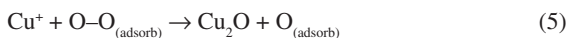
When the dealloying time prolongs to 14 h, as shown in Figure 3b, Cu_2O nanoplates[23] identified by XRD results (Figure 2c) with thickness of 80-90 nm are synthesized by spontaneous oxidation of Cu nanocrystals. With the further increase of the dealloying time (18 h), CuO microwires[26] with diameter of ~2.5 µm are observed in Figure 3c. As a result, designable dealloying products of NPC, Cu_2O, and CuO with interesting morphologies can be tailored in 1.2 M concentrated HCl electrolytes by controlling dealloying time. The surface coverage rate of different

corrosion products with dealloying time is analyzed in Figure 3d, which reveals that Cu crystals could be oxidized into Cu_2O and CuO with different ratio as the extension of the dealloying time. To our knowledge, it is the first time to fabricate Cu_2O nanoplates and CuO microwires in the dealloying and spontaneous oxidation route. We are focusing on controlling the size and productivity of Cu_2O and CuO by adjusting dealloying conditions. With the further development of the dealloying technology, the commercial producing method of Cu_2O and CuO could be extended.

3.3. Chemical process during dealloying

Different kinds of dealloying products are made during etching Cu-Hf-Al metallic glasses in HCl solutions. A clear chemical process[16] can be summarized to explain the diverse types (Cu, Cu_2O and CuO) of these products:

$$Cu_{52.5}Hf_{40}Al_{7.5} + H^+ \rightarrow Cu_{(fresh)} + Hf^{4+} + Al^{3+} + H_2 \quad (1)$$

$$O_{2(dissolve)} = O-O_{(adsorb)} \quad (2)$$

$$Cu_{(fresh)} + 2H^+ = Cu^{2+} + H_2 \quad (3)$$

$$Cu_{(fresh)} + Cu^{2+} = 2Cu^+ \quad (4)$$

$$Cu^+ + O\text{–}O_{(adsorb)} \rightarrow Cu_2O + O_{(adsorb)} \quad (5)$$

$$Cu_2O + O\text{–}O_{(adsorb)} \rightarrow CuO + O_{(adsorb)} \quad (6)$$

Once a Cu-Hf-Al glassy ribbon (Figure 4a) is immersed into HCl electrolytes, the Hf and Al elements are selectively etched, and fresh copper layer is subsequently formed on the surface of the sample (Equation 1 in Figure 4b). As we know, the depth of a dealloyed layer is determined by the dissolution rate of the glassy alloys in HCl solutions besides dealloying time. Usually, the $Cu_{52.5}Hf_{40}Al_{7.5}$ glassy alloy presents very low dissolution rate in diluted HCl solution, whereas it shows enhanced dissolution rate in concentrated HCl solution. In this paper, Figure 1 shows the different particle structure formed on the surface of Cu-Hf-Al glassy substrate when etching in diluted HCl solution. On the other hand, Figure 3a exhibits typical Cu porous structure after dealloying in concentrated HCl solution, which implies that the constituent element Hf in the Cu-Hf-Al alloy shows more active chemical behavior in concentrated HCl solution.
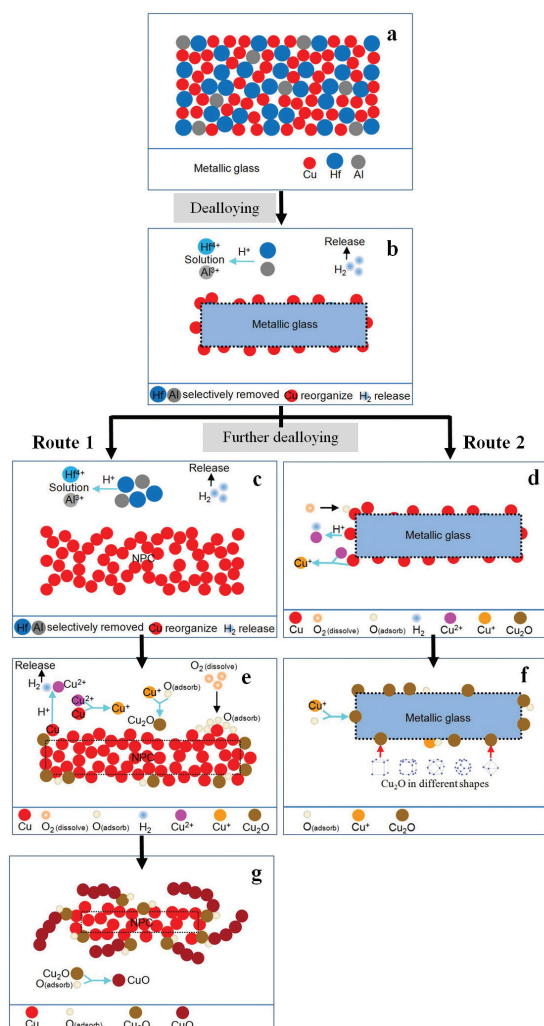

Figure 4. Scheme of the chemical dealloying progress of Cu-Hf-Al glassy alloys under different conditions.

Therefore, the dealloying process in diluted HCl solution might be retarded by the slow dissolution of Hf^{4+} cations or increase of pH value. So, the chemical dealloying process of the Cu-Hf-Al metallic glasses are different between in diluted and concentrated HCl solutions, and can be classified into two routes.

A complete dealloying happens when dealloying in concentrated HCl electrolytes in Figure 4c (Route 1). As a result, the porous structures are formed at the initial stage of the chemical reaction. However, a superficial dealloying happens when dealloying in diluted HCl electrolytes in Figure 4d (Route 2). In this situation, the glassy structures are retained. With the increase of the dealloying time, the Route 1 and Route 2 will further proceed. The oxygen dissolved in the electrolyte is strongly adsorbed on the fresh copper surface (Equation 2). At the same time, part of the fresh Cu dissolves into the acid solutions to form Cu^{2+} cations, acompanying with H_2 release (Equation 3). It seems that it would be easier to form CuO rather than Cu_2O by the reaction of Cu^{2+} cations and adsorbed oxygen. Actually, the Cu^+ cations will be preferentially obtained from a disproportionation reaction between fresh Cu and Cu^{2+} cations (Equation 4). These Cu^+ cations soon react with adsorbed oxygen. As a result, Cu_2O in different shapes are fabricated and heaped up (Equation 5). The creation of Cu_2O during dealloying, which have been reported by other studies[16,20], further confirms the occurrence of the disproportionation reaction in Equation 4. According to different reaction conditions, Cu nanospheres/Cu_2O nanoplates compounds created in Figure 3b are corresponding to Figure 4e in Route 1, while Figure 4f in Route 2 illustrates the formation of the metallic glass/Cu_2O particles in different morphologies (as shown in Figure 1 and Table 1). The key factor for forming Cu_2O crystals with different shapes can be attributed to the value of R[22], which represents the growth rate of Cu_2O particles along the <1 0 0> direction relative to that of the <1 1 1> direction. In this situation, the content (time dependent) of adsorbed oxygen with Cu^+ cations strongly influence the value of R. As a result, Cu_2O crystals with designable shapes can be tailored by controlling dealloying time, as shown in Table 1 and Figure 4f.

Moreover, with the further increase of the dealloying time, Cu_2O is oxidized by adsorbed oxygen on the surface and change to CuO microwires (Equation 6 in Figure 4g). In summary, due to a big difference of examined Cu-Hf-Al alloys in the electrolyte concentration and dealloying time, one or mixed dealloying products (Cu, Cu_2O and CuO), which depend on above chemical process, will finally be produced.

As we know, both Cu_2O and CuO are p-type semiconductors. Cu_2O have potential applications in gas sensors, solar energy conversion, lithium ion batteries, photocatalysts and so on[27-30]. CuO is known for its applications in optical switches, field emitters, gas sensors, Li-ion battery anode materials, and chemical conversion catalysts[31,32]. Hence, Cu_2O and CuO particles with different size and morphologies are highly desirable for wide applications. In traditional chemical method, they are synthesized and stored in liquid solutions. By using

a dealloying process, however, they can be fabricated on solid ribbon and easily stored or extracted from drying oven. According to different application requirement, amorphous/Cu$_x$O[20,21] composites and porous Cu/Cu$_x$O (x=1, 2) composites can be synthesized and tailored by controlling dealloying conditions and choosing different dealloying routes (Figure 4). More detailed studies about applications in various fields of these dealloying products need to be done in the future.

4. Conclusions

In this work, controllable corrosion products are designed by free dealloying Cu-Hf-Al metallic glasses using different technique parameters. The concentration of electrolytes and dealloying time strongly influence the type of dealloying products. A superficial dealloying happens when dealloying in diluted HCl electrolytes. Regular Cu$_2$O microparticles with designable morphology can be tailored in 0.05 M HCl solutions by controlling dealloying time. A complete dealloying take place when dealloying in concentrated HCl electrolytes. Designable products of NPC, Cu$_2$O, and CuO with interesting morphologies are tailored in 1.2 M HCl electrolytes with different dealloying time. A clear chemical process during dealloying is summarized, which guides for designing different useful dealloying products. Due to a big difference of examined Cu-Hf-Al alloys in the electrolyte concentration and dealloying time, one or mixed dealloying products (Cu, Cu$_2$O and CuO), which depend on the progress of relative chemical reactions and the different dealloying route, will finally be produced.

References

1. Farkas D, Caro A, Bringa E and Crowson D. Mechanical response of nanoporous gold. *Acta Materialia*. 2013; 61:3249-3256. http://dx.doi.org/10.1016/j.actamat.2013.02.013

2. Qiu HJ, Kang JL, Liu P, Hirata A, Fujita T and Chen MW. Fabrication of large-scale nanoporous nickel with a tunable pore size for energy storage. *Journal of Power Sources*. 2014; 247:896-905. http://dx.doi.org/10.1016/j.jpowsour.2013.08.070

3. Dan ZH, Qin FX, Sugawara Y, Muto I and Hara N. Elaboration of nanoporous copper by modifying surface diffusivity by the minor addition of gold. *Microporous and Mesoporous Materials*. 2013; 165:257-264. http://dx.doi.org/10.1016/j.micromeso.2012.08.026

4. Wang XG, Tang B, Huang XB, Ma Y and Zhang ZH. High activity of novel nanoporous Pd–Au catalyst for methanol electro-oxidation in alkaline media. *Journal of Alloys and Compounds*. 2013; 565:120-126. http://dx.doi.org/10.1016/j.jallcom.2013.02.170

5. Jia FL, Zhao JH and Yu XX. Nanoporous Cu film/Cu plate with superior catalytic performance toward electro-oxidation of hydrazine. *Journal of Power Sources*. 2013; 222:135-139. http://dx.doi.org/10.1016/j.jpowsour.2012.08.076

6. Tang Y, Tang B, Qing JB, Li Q and Lu LS. Nanoporous metallic surface: Facile fabrication and enhancement of boiling heat transfer. *Applied Surface Science*. 2012; 258:8747-8751. http://dx.doi.org/10.1016/j.apsusc.2012.05.085

7. Detsi E, Sellès MS, Onck PR and Hosson JTMD. Nanoporous silver as electrochemical actuator. *Scripta Materialia*. 2013; 69:195-198. http://dx.doi.org/10.1016/j.scriptamat.2013.04.003

8. Kang JL, Hirata A, Kang LJ, Zhang XM, Hou Y, Chen LY et al. Enhanced supercapacitor performance of MnO$_2$ by atomic doping. *Angewandte Chemie*. 2013; 125:1708-1711. http://dx.doi.org/10.1002/ange.201208993

9. Su LS and Gan YX. Nanoporous Ag and Ag–Sn anodes for energy conversion in photochemical fuel cells. *Nano Energy*. 2012; 1:159-163. http://dx.doi.org/10.1016/j.nanoen.2011.08.002

10. Wittstock A, Biener J and Bäumera M. Nanoporous gold: a new material for catalytic and sensor applications. *Physical Chemistry Chemical Physics*. 2010; 12:12919-12930. http://dx.doi.org/10.1039/c0cp00757a

11. Bringa EM, Monk JD, Caro A, Misra A, Zepeda-Ruiz L, Duchaineau M et al. Are nanoporous materials radiation resistant? *Nano Letters*. 2012; 12:3351-3355. http://dx.doi.org/10.1021/nl201383u

12. Xu CX, Wang RY, Zhang Y and Ding Y. A general corrosion route to nanostructured metal oxides. *Nanoscale*. 2010; 2:906-909. http://dx.doi.org/10.1039/b9nr00351g

13. Xu CX, Liu YQ, Zhou C, Wang L, Geng HR and Ding Y. An in situ dealloying and oxidation route to Co$_3$O$_4$ nanosheets and their ambient-temperature CO oxidation activity. *ChemCatChem*. 2011; 3:399-407. http://dx.doi.org/10.1002/cctc.201000275

14. Hao Q, Li MH, Jia SZ, Zhao XY and Xu CX. Controllable preparation of Co$_3$O$_4$ nanosheets and their electrochemical performance for Li-ion batteries. *RSC Advances*. 2013; 3:7850-7854. http://dx.doi.org/10.1039/c3ra23448g

15. Erlebacher J and Sieradzki K. Pattern formation during dealloying. *Scripta Materialia*. 2003; 49:991-996. http://dx.doi.org/10.1016/S1359-6462(03)00471-8

16. Chen LY, Yu JS, Fujita T and Chen MW. Nanoporous copper with tunable nanoporosity for SERS applications. *Advanced Functional Materials*. 2009; 19:1221-1226. http://dx.doi.org/10.1002/adfm.200801239

17. Li M, Zhou YZ and Geng HR. Fabrication of nanoporous copper ribbons by dealloying of Al-Cu alloys. *Journal of Porous Materials*. 2012; 19:791-796. http://dx.doi.org/10.1007/s10934-011-9532-3

18. Hayes JR, Hodge AM, Biener J, Hamza AV and Sieradzki K. Monolithic nanoporous copper by dealloying Mn–Cu. *Journal of Materials Research*. 2006; 21:2611-2616. http://dx.doi.org/10.1557/JMR.2006.0322

19. Zhao CC, Qi Z, Wang XG and Zhang ZH. Fabrication and characterization of monolithic nanoporous copper through chemical dealloying of Mg–Cu alloys. *Corrosion Science*. 2009; 51:2120-2125. http://dx.doi.org/10.1016/j.corsci.2009.05.043

20. Wang ZF, Qin CL, Zhao WM and Jia JQ. Tunable Cu_2O nanocrystals fabricated by free dealloying of amorphous ribbons. *Journal of Nanomaterials*. 2012; Article ID 126715. http://dx.doi.org/10.1155/2012/126715

21. Wang ZF, Qin CL, Liu L, Wang LJ, Ding J and Zhao WM. Synthesis of $Cu_xO(x = 1,2)$/amorphous compounds by dealloying and spontaneous oxidation method. *Materials Research*. 2014; 17(1):33-37. http://dx.doi.org/10.1590/S1516-14392013005000155.

22. Xu JS and Xue DF. Five branching growth patterns in the cubic crystal system: A direct observation of cuprous oxide microcrystals. *Acta Materialia*. 2007; 55:2397-2406. http://dx.doi.org/10.1016/j.actamat.2006.11.032

23. Kuo CH and Huang MH. Morphologically controlled synthesis of Cu_2O nanocrystals and their properties. *Nano Today*. 2010; 5:106-116. http://dx.doi.org/10.1016/j.nantod.2010.02.001

24. Zhu QW, Zhang YH, Wang JJ, Zhou FS and Chu PK. Microwave synthesis of cuprous oxide micro-/nanocrystals with different morphologies and photocatalytic activities. *Journal of Materials Science & Technology*. 2011; 27:289-295. http://dx.doi.org/10.1016/S1005-0302(11)60064-9

25. Dan ZH, Qin FX, Sugawara Y, Muto I, Makino A and Hara N. Nickel-stabilized nanoporous copper fabricated from ternary TiCuNi amorphous alloys. *Materials Letters*. 2013; 94:128-131. http://dx.doi.org/10.1016/j.matlet.2012.12.028

26. Kim DK, Bae JH, Kang MK and Kim HJ. Analysis on thermite reactions of CuO nanowires and nanopowders coated with Al. *Current Applied Physics*. 2011; 11:1067-1070. http://dx.doi.org/10.1016/j.cap.2011.01.043

27. Zhang JT, Liu JF, Peng Q, Wang X and Li YD. Nearly monodisperse Cu_2O and CuO nanospheres: preparation and applications for sensitive gas sensors. *Chemistry of Materials*. 2006; 18:867-871. http://dx.doi.org/10.1021/cm052256f

28. Mahalingam T, Chitra J, Ravi G, Chu J and Sebastian P. Characterization of pulse plated Cu_2O thin films. *Surface & Coatings Technology*. 2003; 168:111-114. http://dx.doi.org/10.1016/S0257-8972(03)00211-1

29. Poizoy P, Laruelle S, Grugeon S, Dupont L and Trascon J. Nano-sized transition-metal oxides as negative-electrode materials for lithium-ion batteries. *Nature*. 2000; 407:496-499. PMid:11028997. http://dx.doi.org/10.1038/35035045

30. Kumar R, Mastai Y, Diamant Y and Gedanken A. Sonochemical synthesis of amorphous Cu and nanocrystalline Cu_2O embedded in a polyaniline matrix. *Journal of Materials Chemistry*. 2001; 11:1209-1213. http://dx.doi.org/10.1039/b005769j

31. Jiang XC, Herricks T and Xia YN. CuO nanowires can be synthesized by heating copper substrates in air. *Nano Letters*. 2002; 2:1333-1338. http://dx.doi.org/10.1021/nl0257519

32. Grugeon S, Laruelle S, Herrera-Urbina R, Dupont L, Poizot P and Tarascon J. Particle size effects on the electrochemical performance of copper oxides toward lithium. *Journal of The Electrochemical Society*. 2001; 148:A285-A292. http://dx.doi.org/10.1149/1.1353566